

A Study on Flapping Motion for MAV Design

Using Design Exploration

Akira Oyama¹

Japan Aerospace Exploration Agency, Sagami-hara, Kanagawa, 229-8510, Japan

Yoshiyuki Okabe²

University of Tokyo, Sagami-hara, Kanagawa, 229-8510, Japan

Kozo Fujii³

Japan Aerospace Exploration Agency, Sagami-hara, Kanagawa, 229-8510, Japan

and

Koji Shimoyama⁴

Japan Aerospace Exploration Agency, Sagami-hara, Kanagawa, 229-8510, Japan

Aerodynamic knowledge for practical flapping-wing micro air vehicle (MAV) design is obtained by application of the design exploration framework coupled with CFD to a multiobjective aerodynamic design optimization problem of two-dimensional flapping motion of an airfoil. Lift and thrust are maximized while required power is minimized in the design problem. Pareto-optimal solutions are obtained by a multiobjective evolutionary optimization and analyzed with the self-organizing map. Aerodynamic performance of each flapping motion is evaluated by a two-dimensional Navier-Stokes solver. The result reveals tradeoff information between each objective and effect of each design parameters on them. Analysis of the time histories of lift, thrust, and required power coefficients and corresponding pressure coefficient distribution of the extreme Pareto-optimal solutions leads to useful guidelines for the lift maximization, thrust maximization, and required power minimization.

Nomenclature

C	=	airfoil chord
$C_L(t)$	=	lift coefficient
$C_T(t)$	=	thrust coefficient
$C_M(t)$	=	moment coefficient
$C_{PR}(t)$	=	required power coefficient
h	=	plunge amplitude nondimensionalized with c
f	=	flapping frequency, Hz
k	=	reduced frequency, $2\pi fc / U_\infty$

¹ Research Associate, Department of Space Transportation Engineering, Institute of Space and Astronautical Science, 3-1-1 Sagami-hara Kanagawa Japan, AIAA Member.

² Graduate Student, Department of Aeronautics and Astronautics, 3-1-1 Sagami-hara Kanagawa Japan, currently Mitsubishi Heavy Industries, LTD.

³ Professor, Department of Space Transportation Engineering, Institute of Space and Astronautical Science, 3-1-1 Sagami-hara Kanagawa Japan, AIAA Fellow.

⁴ Graduate Student, Department of Aeronautics and Astronautics, 3-1-1 Sagami-hara Kanagawa Japan, Currently Institute of Fluid Science, Tohoku University, AIAA Member.

L	= lift
N	= normal aerodynamic force
P	= power
q	= dynamic pressure, $0.5\rho U_\infty^2$
St	= Strouhal number, $kh/2\pi$
t	= time nondimensionalized with U_∞ and c
T	= thrust
U_∞	= freestream velocity
$x(t)$	= horizontal position nondimensionalized with airfoil chord
$y(t)$	= vertical position nondimensionalized with airfoil chord
$\alpha(t)$	= pitch angle
α_0	= pitch angle offset
α_1	= pitch angle amplitude
$\alpha_e(t)$	= effective angle of attack
η	= propulsive efficiency, C_T/C_{PR}
ϕ	= phase shift

Subscript

Ave = time-averaged value over one flapping cycle

I. Introduction

Research Interest in flapping wings in aerospace engineering recently increases as flapping wing system may be more suitable for micro air vehicles (MAVs) than fixed wing system at low Reynolds number. For the development of MAV with flapping wings, understanding of aerodynamic mechanism of a flapping wing for higher aerodynamic performance in terms of lift, thrust, and efficiency is important. Garrick¹ estimated thrust and propulsive efficiency of plunging or pitching airfoil using incompressible potential flow analysis. He demonstrated that thrust is proportional to square of frequency and square of plunge amplitude. Tuncer and Platzer² performed Navier-Stokes computations of an oscillating airfoil, where the propulsive efficiency is found to be a strong function of reduced frequency and the plunge amplitude. Isogai et al.³ performed parametric study of an airfoil oscillating in coupled mode (pitching and plunging) using Navier-Stokes simulations, where highest efficiency was achieved in the case the pitching oscillation advances 90 degrees ahead of the plunging oscillation and the reduced frequency is at some optimum value. Tuncer and Kaya⁴ optimized thrust and/or propulsive efficiency of an oscillating airfoil using a gradient-based method coupled with a Navier-Stokes solver where design parameters are pitch and plunge amplitudes and the phase shift between the pitch and plunge motions. They demonstrated that there is tradeoff between maximizations of thrust and propulsive efficiency and effective angle of attack is to be reduced for a high propulsive efficiency to prevent large-scale leading edge separation. Anderson et al.⁵ experimentally showed that the phase angle shift between pitch and plunge oscillations have strong effect on propulsive efficiency.

While studies in the past have given significant insight into understanding of aerodynamic mechanism of a flapping wing, most of them considered only maximization of thrust and propulsive efficiency. Previous discussions on tradeoff between thrust and propulsive efficiency were intricate because propulsive efficiency is a function of the thrust itself. For example, higher thrust turns out to be higher propulsive efficiency even if the used power is constant. Thus, in addition to thrust, required power instead of propulsive efficiency should be considered for easier understanding of the flapping mechanism. Past studies also have not discussed relationship between these aerodynamic performances and lift, which is an important aerodynamic index as it determines vehicle, payload, and fuel weights. In fact, the flapping motion design is a typical multiobjective design optimization problem that has three contradicting objectives; maximization of thrust, maximization of lift, and minimization of required power.

Recently, idea of ‘design exploration’ was proposed as a tool to extract essential knowledge from multiobjective optimization problem such as tradeoff information between contradicting objectives and effect of each design parameter on the objectives. In the framework of design exploration, Pareto-optimal solutions are obtained by multiobjective optimization using such as multiobjective evolutionary algorithm⁶ and then important design knowledge is extracted by analyzing the obtained Pareto-optimal solutions using so-called data mining approaches such as self-organizing map⁷ and analysis of variance⁸. Obayashi et al. applied the idea of design exploration to understand fly-back booster of reusable launch vehicle design and regional-jet wing design and got some practically import design knowledge⁹.

The objective of the present study is to extract aerodynamic knowledge on the flapping motion such as 1) tradeoff information between lift, thrust, and required power, 2) effect of flapping motion parameters such as plunge amplitude and frequency, pitching angle amplitude and offset, and phase difference on the objective functions, and to create guidelines for the design of flapping motion for lift maximization, thrust maximization and required power minimization. To obtain such knowledge, the design exploration framework is applied to a multiobjective aerodynamic design optimization problem of a flapping airfoil for a MAV for Mars exploration where lift and thrust are maximized and required power is minimized. The aerodynamic performance and required power are evaluated with the numerical simulations of the two-dimensional incompressible Navier-Stokes equations. Multiobjective evolutionary algorithm and self-organizing map are used to explore the design problem.

II. Design Optimization Problem

Flapping airfoil for the MAV discussed in the United States for future Mars exploration^{10,11} is considered. This MAV has a span length of 1 [m] and chord length of 0.1 [m]. Its cruising speed is more than 10 [km/hour] and the cruising Reynolds number based on Mars air properties and reference length of the chord is assumed to be 10^3 . Note that the results are applicable to MAV on the earth because the Reynolds number is only the non-dimensional parameter that represents Mars atmosphere in this study.

The objectives are maximization of the time-averaged lift and thrust coefficients and minimization of the time-averaged required power coefficient at its cruising condition, where the lift, thrust, and required power are averaged over one flapping cycle:

$$C_{L,ave} = f \cdot \int_{t=0}^{1/f} C_L(t) dt \quad (1)$$

$$C_{T,ave} = f \cdot \int_{t=0}^{1/f} C_T(t) dt \quad (2)$$

$$C_{PR,ave} = f \cdot \int_{t=0}^{1/f} C_{PR}(t) dt \quad (3)$$

where

$$C_{PR}(t) = -\left(\frac{dy(t)}{dt} \cdot C_L(t) + \frac{d\alpha(t)}{dt} \cdot C_M(t)\right) \quad (4)$$

Constraints are applied on averaged lift and thrust coefficients so that they are positive. The airfoil is assumed to be NACA 0002 airfoil. The flapping motion of the airfoil (see Fig. 1) is expressed by plunging and pitching motions as:

$$y(t) = h \cdot \sin(kt) \quad (5)$$

$$\alpha(t) = \alpha_0 \sin(kt + \phi) + \alpha_1 \quad (6)$$

where design parameters are h , k , α_0 , α_1 , and ϕ . The present design space is shown in Table 1.

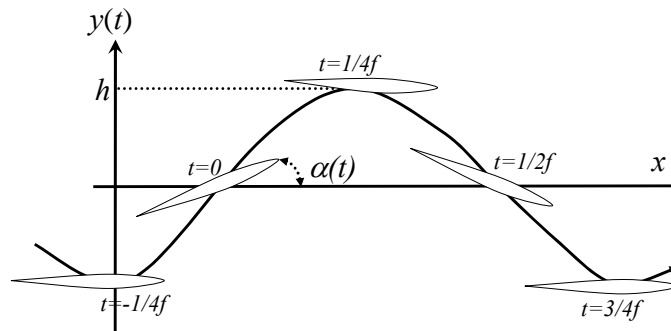


Figure 1. Parameterization of flapping motion.

Table 1. Design space

Design parameters	lower boundary	upper boundary
Reduced frequency k	0.2	0.9
Plunge amplitude h	0.5	2.2
Pitch amplitude α_1	10[deg]	45[deg]
Pitch offset α_0	0 [deg]	30[deg]
Phase shift ϕ	70[deg]	110[deg]

III. Aerodynamic Force Evaluation

The two-dimensional incompressible Navier-Stokes equations and the continuity equation on the generalized curvilinear coordinates are solved using pseudo-compressible flow simulation approach. The dual-time stepping procedure¹², which allows an implicit method to be used in real time with the updated solution obtained through sub-iterations in pseudo-time, is employed. The numerical fluxes are evaluated by the Roe scheme¹³ where physical properties at the grid interface are evaluated by the MUSCL interpolation¹⁴ based on primitive variables. The viscous terms are evaluated by second-order central differencing scheme. Lower-upper symmetric Gauss-Seidel (LU-SGS) factorization implicit algorithm¹⁵ is used for the time integration. Note that the original version of the program for compressible flow analysis has been used for a wide variety of CFD studies.¹⁶⁻¹⁸

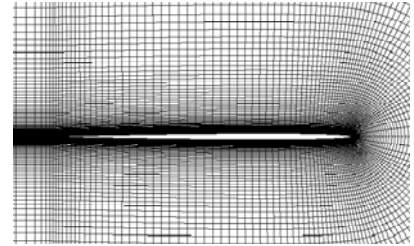


Figure 2. Close-up view of the computational grid near the airfoil.

The corresponding computational grid is a C-type grid (Fig. 2) that has 201 (chordwise direction) x 101 (normal direction) grid size. Number of time steps for each flapping cycle is 1,700. Grid and time step size convergence have been confirmed to be enough for qualitative discussion. Averaged lift and thrust coefficients and required power are obtained for the third flapping cycle.

The freestream flow conditions are applied to the inflow boundary. The outer boundary of the computational domain is placed at twenty chord length away from the leading edge of the airfoil. On the outflow boundary, pressure is fixed to the freestream value while the other physical properties are extrapolated from the corresponding interior grid points. The airfoil surface is treated as non-slip wall boundary. Physical properties on the wake boundary are interpolated from the adjacent grid points. The initial condition is the uniform flow.

IV. Design Optimization

Objective of the present study is to present aerodynamic knowledge for researchers or designers of flapping wing MAV from the multiobjective MAV design problem. To extract such information, it is necessary to obtain the Pareto-optimal solutions of the multiobjective design optimization problem, which are all optimal in the sense that no other solutions in the search space are superior to them when all objectives are considered, and to analyze them with data mining approach such as self-organizing map.

Traditional methods such as gradient-based methods are basically single-objective optimization method. When such method is applied to a multiobjective optimization problem, the problem is converted to a single-objective design optimization problem by combining the multiple objectives into a single objective typically using a weighted sum method. This approach can find only one of the Pareto-optimal solutions corresponding to the user-specified weight coefficients. Hence, a multiobjective design optimization method is required for the present study.

Multiobjective evolutionary algorithm (MOEA, for example, see Ref. 6) is an optimization algorithm mimicking mechanism of the natural evolution, where a biological population evolves over generations to adapt to an environment by selection, recombination and mutation. MOEA has multiobjective optimization nature thanks to its population-based search algorithm toward higher fitness regions where fitness is determined through Pareto-ranking and fitness sharing. In addition, MOEA has some other advantages over traditional approaches such as:

- 1) Suitability to real world design optimization problems: Because MOEA does not use function gradients, MOEA is suitable to real world design optimization problems which usually involve non-differentiable/multimodal objective function and/or a mix of continuous, discrete, and integer design parameters.

- 2) Suitability to parallel computing environment: Since MOEA is a population-based search algorithm, all design candidates in each generation can be evaluated in parallel by using the simple master-slave concept. Parallel efficiency is also very high, if objective function evaluations consume most of CPU time. Aerodynamic optimization using computational fluid dynamics (CFD) is a typical case.
- 3) Simplicity in coupling CFD codes: As MOEA uses only objective/constraint function values of design candidates, MOEA does not need substantial modification or sophisticated interface to the CFD code. If an all-out re-coding were required to every optimization problem, like the adjoint methods, extensive validation of the new code would be necessary every time. MOEA can avoid such troubles.

These features are essential for knowledge extraction from the present multiobjective optimization problem. Therefore, the MOEA presented in the next section is used to obtain the Pareto-optimal solutions of the present flapping motion design optimization problem.

A. Present Multiobjective Evolutionary Algorithm

As MOEA originally simulated natural evolution, traditional MOEA treats design parameters represented by binary numbers. However, for real design parameter optimizations such as the present aerodynamic optimization problem, it is more straightforward to use real numbers. Thus, the present design parameters h , k , α_o , α_s , and ϕ are represented by real numbers.

Flowchart of the present MOEA is illustrated in Fig. 3. The population size is kept at thirty-two and the maximum number of generations is set to fifty. The initial population is generated randomly so that the initial population covers entire design space presented in Table 1.

Values of the present objective and constraint functions C_L , C_T , and C_{PR} of each design candidate are evaluated through CFD described in the section 3 and fitness of each design candidate is computed according to Pareto-ranking, fitness sharing, and Pareto-based constraint handling¹⁹ based on its objective function and constraint function values. Here, Fonseca and Fleming's Pareto-based ranking method²⁰ and fitness sharing method²⁰ are used for Pareto-ranking where each individual is assigned a rank according to the number of individuals dominating it. In Pareto-based constraint handling, rank of feasible designs is determined by Pareto-ranking based on the objective function values while rank of infeasible designs is determined by Pareto-ranking based on the constraint function values.

Parents of new generation are selected through roulette selection²¹ from the best thirty-two individuals among the present generation and the best thirty-two individuals in the previous generation.

New generation is reproduced through crossover and mutation operators. Crossover is an operator which combines genotype of the selected parents and produces new individuals with the intent of improving the fitness value of the next generation. Here, the blended crossover²² where α of 0.5 is used for crossover between the selected solutions. Mutation is applied to the design parameters of the new generation to maintain diversity. Here, mutation takes place at a probability of 20% and then adds a random disturbance to the corresponding gene up to 10% of the given range of each design parameter.

Evaluation process at each generation is parallelized using the master-slave concept; where the grid generations and the flow calculations associated to the individuals of a generation are distributed into 32 processing elements of the JAXA/ISAS NEC SX-6 computing system. This makes the corresponding turnaround time almost 1/32 because the CPU time used for MOEA operators are negligible. Total turn around time of the present optimization is roughly nine hours.

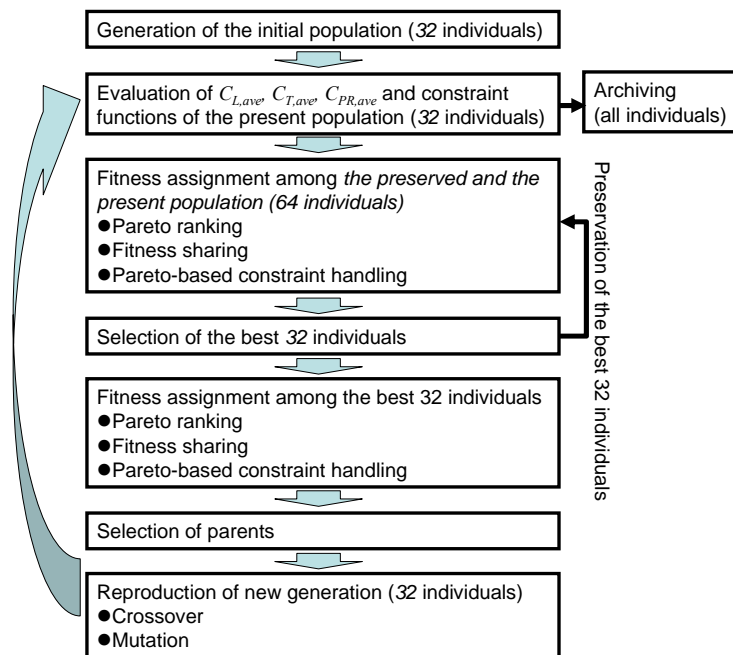


Figure 3. Flowchart of the present MOEA.

V. Data Mining

If an optimization problem has two objective functions, tradeoff relation between them as well as effect of each design parameter can be easily understood through a two-dimensional plotting. On the contrary, understanding the tradeoff relations and effect of design parameters involving three or more objective functions is not straightforward. Kohonen's self-organizing map (SOM)⁷ is used to analyze the Pareto-optimal solutions in the present study.

SOM is an artificial neural network where all the solutions are aligned on a grid according to Kohonen algorithm so that neighboring nodes are similar to each other. Mostly, SOM is used for nonlinear projection of input data in three or higher dimensional space onto two-dimensional space to extract knowledge implicit in data such as attributes and features.

A software package called Viscovery SOMine plus 4.0²³ produced by Eudaptics GmbH is used. Although SOMine is based on the general SOM concept and algorithm, it employs an advanced variant of unsupervised neural networks, i. e., Kohonen's Batch SOM, which is a more robust approach due to its mediation over a large number of learning steps.

Here, the Pareto-optimal solutions distributed in the present three-dimensional objective function space (C_L maximization, C_T maximization, and C_{PR} minimization) are mapped into nodes on a two-dimensional grid according to the similarity in terms of the objective function values. Then the two-dimensional map colored according to each objective function, each design parameter, propulsion efficiency, and Strouhal number are compared for the knowledge acquisition from the present problem.

VI. Results and Discussion

The Pareto-optimal flapping motions (shown by spheres) and all the other solutions obtained by the present optimization (shown by circles) are plotted in the three-dimensional objective function space (Fig. 4). Tradeoff among the maximization of the averaged lift and thrust and minimization of the averaged required power is observed. However, it is very difficult to understand effect of each design parameter on the tradeoff in the three-dimensional plot. In 6.1, the Pareto-optimal solutions are analyzed more in detail with SOM. Then, in 6.2, flapping mechanism of the extreme Pareto-optimal solutions i. e., lift-maximum, thrust-maximum, required-power-minimum solutions (presented in Table 2) is investigated in detail.

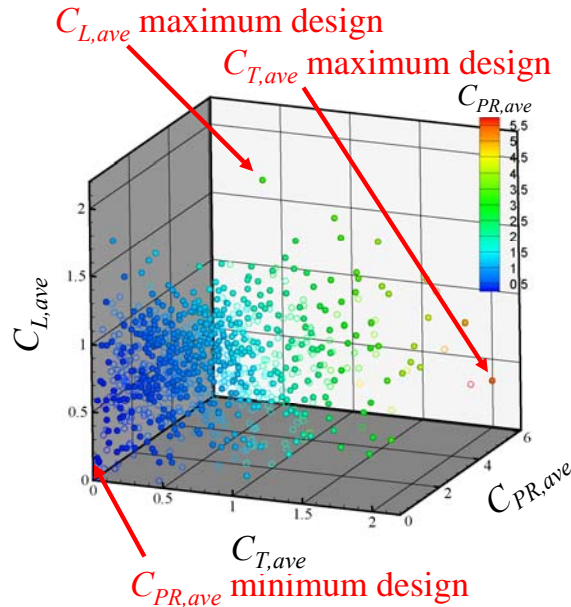


Figure 4. Evaluated flapping motions (circles) and obtained Pareto-optimal solutions (spheres) plotted in the objective function space.

Table. 2 Objective function and design variable values of the extreme Pareto-optimal solutions.

	Maximum thrust flapping	Maximum lift flapping	Minimum required power flapping
$C_{T,ave}$	2.09	0.77	0.03
$C_{L,ave}$	0.42	1.97	0.13
$C_{PR,ave}$	5.42	3.27	0.09
Reduced frequency k	0.88	0.80	0.46
Plunge amplitude h	2.10	2.06	1.88
Pitch amplitude α_l	38.2 [deg]	34.9 [deg]	37.7 [deg]
Pitch offset α_o	3.53 [deg]	21.2 [deg]	1.18 [deg]
Phase shift ϕ	94.0 [deg]	90.4 [deg]	85.5 [deg]

A. Data Mining Using SOM

The Pareto-optimal solutions in the three-dimensional objective function space (shown in Fig. 4) are mapped into nodes on a two-dimensional grid where neighboring nodes are similar to each other in terms of objective function values. It should be noted that direction and Euclidean distance in the objective function space are lost on the SOM. Figure 5 presents the obtained SOM where each node is colored according to each objective function value. Flapping motions for smaller required power were mapped on right side of the SOM while those for larger lift or thrust were distributed on left side of the SOM. This figure indicates the tradeoff between the three objectives and there is no solution that optimizes all three objectives simultaneously. This figure also indicates that maximizing thrust requires more power than maximizing lift.

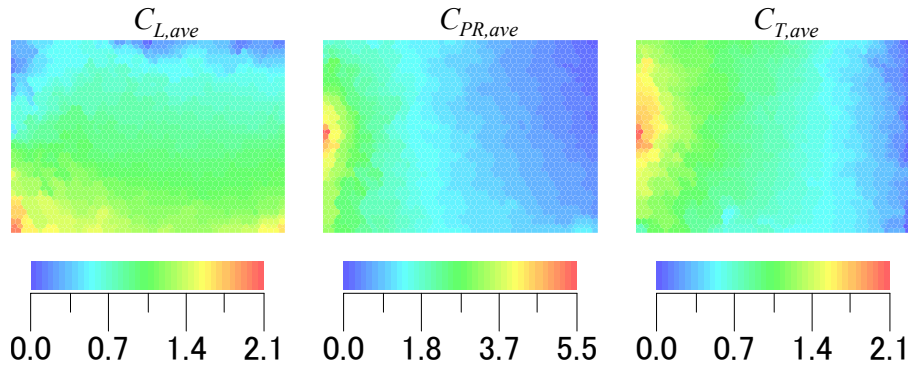


Figure 5. SOM colored according to each objective function.

The same SOM colored according to propulsive efficiency and Strouhal number is presented in Fig. 6. According to the research by Taylor et al.²⁴, flying animals such as birds, bats and insects in cruise flight operate within a narrow range of Strouhal number between 0.2 and 0.4. Also, Young demonstrated some Navier-Stokes computations to show propulsive efficiency has a peak around a Strouhal number of 0.2.²⁵ Strouhal number of the obtained flapping motions is consistent with these results.

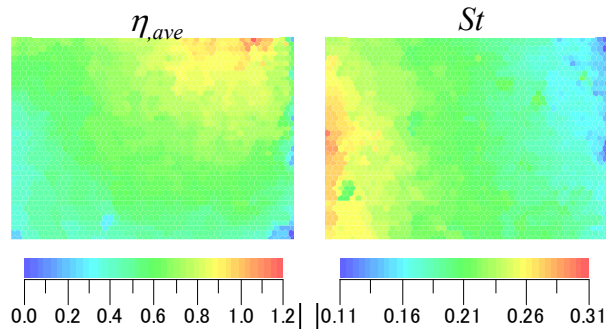


Figure 6 SOM colored according to propulsive efficiency and Strouhal number.

Comparison between distributions of lift and propulsive efficiency in the Figs. 5 and 6 indicates that lift should be minimized for maximum propulsive efficiency, which is natural because it is necessary to use generated aerodynamic force for thrust production as much as possible to increase propulsive efficiency. Propulsive efficiency was maximized at a certain point between maximum of thrust and minimization of required power. These figures also show that St becomes smaller as required power becomes smaller while it becomes larger as thrust or lift becomes larger.

The same SOM colored according to each design parameter value is presented in Fig. 7. Comparison between Figs. 5 and 7 gives additional knowledge on the design optimization problem;

- 1) Phase shift between plunging and pitch angle cycles of the obtained Pareto-optimal solutions are almost ninety degrees. This result is consistent with previous researches on flapping motion such as Ref. 3 where efficiency became high when pitch leads plunging by about 90 degrees.
- 2) Pitch angle offset has strong influence on the lift coefficient. As pitch angle offset becomes higher, lift becomes larger. Pitch offset of most of the Pareto-optimal solutions are between 0 degree to 10 degrees.
- 3) Frequency seems to be a tradeoff parameter between minimization of required power and maximization of lift or thrust where smaller frequency leads to smaller required power.
- 4) Plunge amplitude largely influences on thrust where higher plunge amplitude leads to larger thrust. This result is consistent with previous research results such as Ref. 1. The result that most of the Pareto-optimal solution have plunge amplitude of 18 to 2.2 also indicates that certain level of plunge amplitude is necessary.

Pitch angle amplitude of the most Pareto-optimal solutions were between 35 and 45 degrees, which indicates that certain level of pitch angle amplitude is also necessary for high performance flapping motion. This figure also indicates that better solutions may have been found if the search space was wider since 45 degrees is upper limit of the present search space of α_1 .

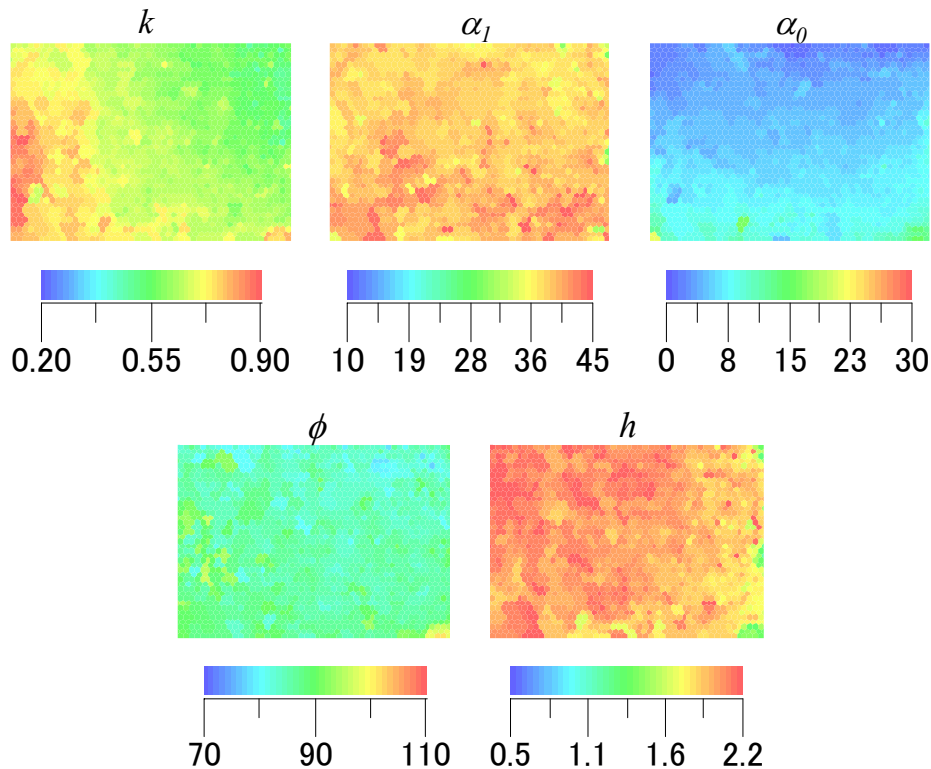


Figure 7. SOM colored according to each design parameter.

B. Analyses of the extreme Pareto-Optimal Solutions

1. Flapping Motion for Maximum Thrust

Time histories of vertical position, pitch angle, effective angle of attack, and lift, thrust, required power coefficients of the maximum thrust flapping motion are presented in Fig. 8. This figure indicates that flapping motion for maximum thrust had large absolute effective angle of attack to produce large aerodynamic force in down stroke motion as well as up stroke motion, which generates large lift and thrust in down stroke motion and large negative lift and positive thrust in up stroke motion. Corresponding pressure coefficient distribution shown in Fig. 9 indicates that the up stroke motion produces a strong vortex separated from the leading edge to generate large thrust while the down stroke motion produces a strong vortex separated from the leading edge for large thrust and lift.

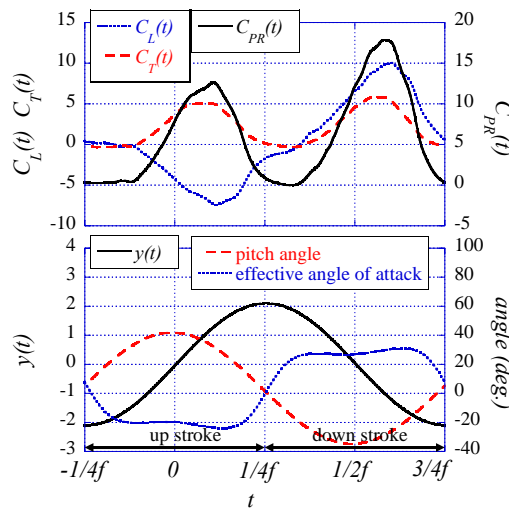


Figure 8. Time histories of position, pitch angle, effective angle of attack, and the aerodynamic coefficients of the thrust maximum flapping motion.

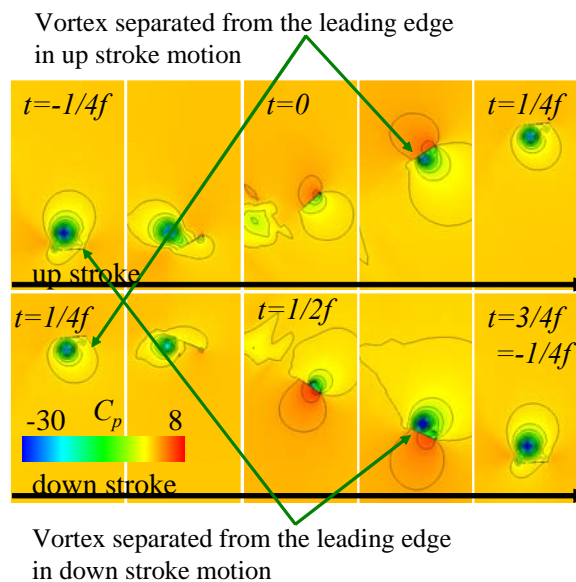


Figure 9. Pressure coefficient distribution around the thrust maximum flapping motion.

2. Flapping Motion for Maximum Lift

Time histories of vertical position, pitch angle, effective angle of attack, and lift, thrust, required power coefficients of the maximum lift flapping motion are presented in Fig. 10. The effective angle of attack is almost zero in up stroke motion while it is more than forty degrees in down stroke motion. As a result, lift maximum flapping motion generates small lift and thrust in up stroke motion while it generates very large lift in down stroke motion. Corresponding pressure coefficient distribution is presented in Fig. 11. It is interesting that the flapping motion for maximum lift generates additional vortex separated from the trailing edge in down stroke motion for large lift.

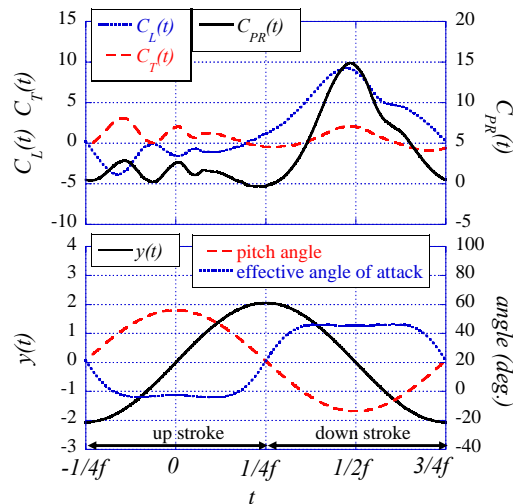


Figure 10. Time histories of position, pitch angle, effective angle of attack, and the aerodynamic coefficients of the lift maximum flapping motion.

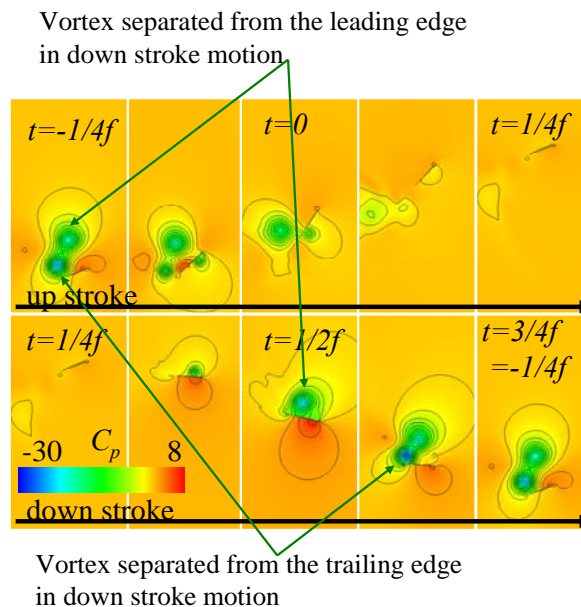


Figure 11. Pressure coefficient distribution around the lift maximum flapping motion.

3. Flapping Motion for Minimum Required Power

Time histories of vertical position, pitch angle, effective angle of attack, and lift, thrust, required power coefficients of the minimum required power flapping motion are presented in Fig. 12. In contrast to the previous extreme flapping motions, the flapping motion for minimum required power maintain almost zero effective angle of attack to minimize required power in both up and down stroke motions. Corresponding pressure coefficient distribution is presented in Fig. 13.

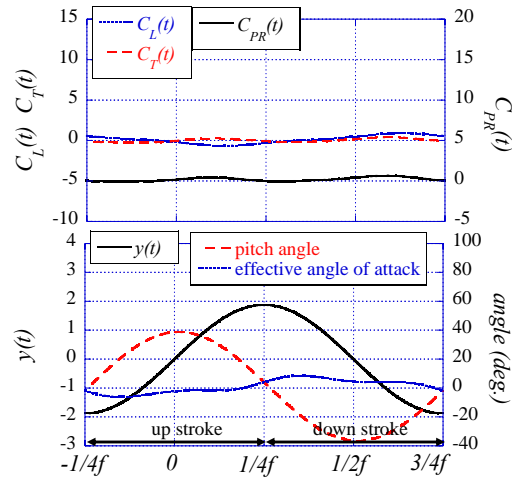


Figure 12. Time histories of position, pitch angle, effective angle of attack, and the aerodynamic coefficients of the required power minimum flapping motion.

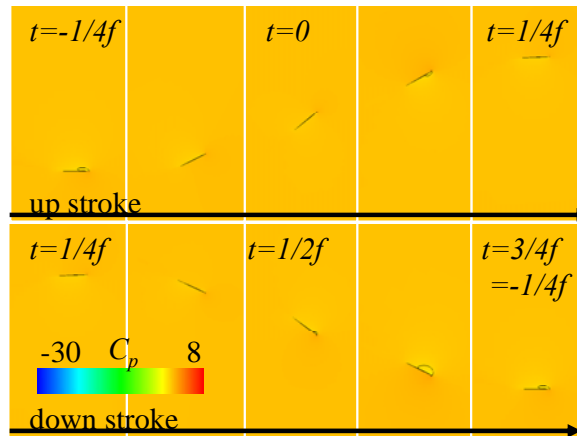


Figure 13. Pressure coefficient distribution around the required power minimum flapping motion.

VII. Conclusions

The design exploration framework has been applied to a multiobjective aerodynamic design optimization problem of a two-dimensional flapping motion to obtain aerodynamic knowledge for practical flapping-wing MAV design. To explore the design problem, the Pareto-optimal solutions obtained by a multiobjective evolutionary algorithm were analyzed with the self-organizing map and the time histories of lift, thrust, and required power coefficients and corresponding pressure coefficient distribution of the extreme Pareto-optimal solutions were discussed.

Analysis of the objective function values of the Pareto-optimal solutions using SOM showed tradeoff between thrust maximization, lift maximization and required power minimization. Analysis of the design variables of the Pareto-optimal solutions using SOM led to some knowledge on aerodynamic flapping mechanism;

- 1) phase shift between plunging and pitch angle cycles of the obtained Pareto-optimal solutions is almost ninety degrees.
- 2) pitch angle offset has strong influence on the lift coefficient.
- 3) frequency seems to be a tradeoff parameter between minimization of required power and maximization of lift or thrust where smaller frequency leads to smaller required power.
- 4) plunge amplitude largely influences on thrust where higher plunge amplitude leads to larger thrust.

Examination of the extreme Pareto-optimal solutions indicated;

- 1) the obtained flapping motion for maximum thrust generates large positive thrust and large negative lift in up stroke motion while it generates large positive thrust and lift in down stroke motion.
- 2) the obtained flapping motion for maximum lift generates small thrust and lift in up stroke motion while it generates large positive lift in down stroke motion.
- 3) the obtained flapping motion for minimum required power generates small thrust and lift in both up stroke and down stroke motions.

Also the present results indicate that those aerodynamic forces are largely due to vortex generation both from the leading edge and the trailing edge.

The present result ensured that the design exploration framework coupled with CFD is useful approach for real world design optimization problems. Though the present demonstration was MAV design for Mars exploration, the aerodynamic knowledge extracted from the present study should be useful for designers of flapping-wing MAV for Earth air as long as Reynolds number and cruising speed is almost same.

References

- ¹Garrick, I. E., "Propulsion of a Flapping and Oscillating Airfoil," NACA Report 567, 1936.
- ²Tuncer, I. H., and Platzer, M. F., "Thrust Generation Due to Airfoil Flapping," *AIAA Journal*, Vol. 34, No. 2, 1995, pp. 324-331.
- ³Isogai, K., Shinmoto, Y., and Watanabe, Y., "Effects of Dynamic Stall on Propulsive Efficiency and Thrust of Flapping Airfoil," *AIAA Journal*, Vol. 37, No. 10, 1999, pp. 1145-1151.
- ⁴Tuncer, I. H., and Kaya, M., "Optimization of Flapping Airfoils for Maximum Thrust and Propulsive Efficiency," *AIAA Journal*, Vol. 43, No. 11, 2005, pp. 2329-2336.
- ⁵Anderson, J. M., Streitlien, K., Barrett D.S., and Triantafyllou, M. S., "Oscillating Foils of High Propulsive Efficiency," *Journal of Fluid Mechanics*, Vol. 360, Issue 01, 1998, pp. 41-72.
- ⁶Deb, K., *Multi-Objective Optimization Using Evolutionary Algorithms*, John Wiley & Sons, Ltd., Chichester, UK, 2001.
- ⁷Kohonen, T., *Self-Organizing Maps*, Second edition, Springer, Heidelberg, Germany, 1997.
- ⁸Donald, R. J., Matthias, S., and William, J. W., "Efficient Global Optimization of Expensive Black-Box Function," *Journal Global Optimization*, Vol. 13, 1998, pp. 455-492.
- ⁹Obayashi, S., Jeong, S., and Chiba, K., "Multi-Objective Design Exploration for Aerodynamic Configurations," AIAA Paper 2005-4666, 2005.
- ¹⁰URL: <http://avdil.gtri.gatech.edu/RCM/RCM/Entomopter/EntomopterProject.html>
- ¹¹Michielson, R. C., and Reece, S., "Update on Flapping Wing Micro Air Vehicle Research on Going Work to Develop a Flapping Wing, Crawling "Entomopter"," *Proceedings of the 13th Bristol International RPV Conference*, 1998.
- ¹²Jameson, A., "Time Dependent Calculations Using Multigrid, with Applications to Unsteady Flows Past Airfoils and Wings," AIAA Paper 1991-1596, 1991.
- ¹³Roe, P. L., "Approximate Riemann Solvers, Parameter Vectors, and Difference Schemes," *Journal of Computational Physics*, Vol. 43, 1981, pp. 357-372.
- ¹⁴van Leer, B., "Towards the Ultimate Conservative Difference Scheme. A Second-Order Sequel to Godunov's Method," *Journal of Computational Physics*, Vol. 32, 1979, pp. 101-136.
- ¹⁵Yoon, S., and Jameson, A., "Lower-Upper Symmetric-Gauss-Seidel Method for the Euler and Navier-Stokes Equations," *AIAA Journal*, Vol. 26, No. 9, 1988, pp. 1025-1026.

- ¹⁶Ito, T., Fujii, K., and Hayashi, K., "Computations of Axisymmetric Plug-Nozzle Flowfields: Flow Structures and Thrust Performance," *Journal of Propulsion and Power*, Vol. 18, No. 2, 2002, pp. 254-260.
- ¹⁷Kawai, S., and Fujii, K., "Analysis and Prediction of Thin-Airfoil Stall Phenomena with Hybrid Turbulence Methodology," *AIAA Journal*, Vol. 43, No. 5, 2005, pp. 953-961.
- ¹⁸Fujimoto, K., and Fujii, K., "Computational Aerodynamic Analysis of Capsule Configurations Toward the Development of Reusable Rockets," *Journal of Spacecraft and Rockets*, Vol. 43, No. 1, 2006, pp. 77-83.
- ¹⁹Oyama, A., Shimoyama, K., and Fujii, K., "New constraint-handling method for multi-objective multi-constraint evolutionary optimization," *Transactions of JSASS*, 2007, (in press).
- ²⁰Fonseca, C. M., and Fleming, P. J., "Genetic Algorithms for Multiobjective Optimization: Formulation, Discussion and Generalization," *Proceedings of the 5th international conference on genetic algorithms*, edited by Forrest, S., Morgan Kaufmann Publishers, Inc., San Mateo, CA, 1993, pp. 416-423.
- ²¹Goldberg, D. E., *Genetic algorithms in search, optimization and machine learning*, Addison-Wesley Publishing Company, Inc., Reading, MA, 1989.
- ²²Eshelman, L. J., and Schaffer, J. D., "Real-coded Genetic Algorithms and Interval Schemata," *Foundations of genetic algorithms 2*, edited by Whitley, L. D., Morgan Kaufmann Publishers, Inc., San Mateo, CA, 1993, pp. 187-202.
- ²³Eudaptics, URL:<http://www.eudaptics.com>.
- ²⁴Taylor, G. K., Nudds, R. L., and Thomas, A. L. R., "Flying and Swimming Animals Cruise at a Strouhal Number Tuned for High Power Efficiency," *Nature*, 2003, Vol. 425, pp. 707-711.
- ²⁵Young, J., "Numerical Simulation of the Unsteady Aerodynamics of Flapping Airfoils," Ph.D. Dissertation, Australian Defense Force Academy, 2005.